

Proton Structure and PHENIX Experiment

Jian-Wei Qiu^{1,2}

*Department of Physics, Brookhaven National Laboratory, Upton, NY 11973, USA C.N. Yang
Institute for Theoretical Physics and Department of Physics and Astronomy, Stony Brook
University, Stony Brook, NY 11794, USA*

**E-mail: jqiu@bnl.gov*

.....
We briefly summarize the important and critical roles that PHENIX Experiment has played in determining the proton's internal structure in terms of quarks and gluons, and their dynamics. Some pioneering measurements by PHENIX Experiment on the motion and polarization of quarks and gluons, as well as their correlations inside a fast moving proton are presented. Some future opportunities and potentials of PHENIX Experiment are also discussed.
.....

Subject Index QCD, Proton Structure, PHENIX

1. Introduction

Proton, along with neutron, known as the nucleon, is the fundamental building block of all atomic nuclei that make up all visible matter in the universe, including the stars, planets, and us. Proton is also known as a strongly interacting, relativistic bound state of quarks and gluons (referred as partons) in Quantum Chromo-Dynamics (QCD) [1]. In order to explain the origin, the evolution, and the structure of the visible world, it is necessary to explore and to understand the proton's internal structure and its formation.

The advances of accelerator technology in the last century made it possible to discover the quarks, the fundamental constituents of the proton, in the nineteen sixties at Stanford Linear Accelerator Center (SLAC) [2, 3], which led to the discovery of QCD. QCD is the theory of strong interacting color charges that is responsible for binding colored quarks into the color neutral proton by the exchange of gluons [4]. In contrast to the quantum electromagnetism, where the force carrying photons are electrically neutral, the force carrying gluons in QCD carry the color charge causing them to interact among themselves, which is the defining property of QCD responsible for the complex and extremely rich, while mysterious structure of the proton, and the countless intriguing phenomena of strong interaction physics.

Proton structure is not static, but, dynamic, full of features beyond our current knowledge and imagination. Quarks and gluons interact strongly when they are far apart – the confinement of color, but, weakly when they are closer – the Asymptotic Freedom; they appear and disappear in numbers almost continuously; and they are confined to form the proton while moving relativistically [1]. Understanding completely the proton structure and its properties (such as its mass, spin, size, and etc.), the emergent phenomena of QCD dynamics, is still beyond the capability of the best minds in the world today. It is the great intellectual challenge to explore and to understand the proton structure and its properties without being able to see the quarks and gluons in isolation.

Relativistic heavy ion collider (RHIC) at Brookhaven National Laboratory (BNL) was the first collider facility in the world to be able to perform experiments with the collisions of two relativistic heavy ion beams, as well as two polarized proton beams [5]. From collisions of two gold ion beams, RHIC discovered, later confirmed by the experiments at the Large Hadron Collider (LHC) at CERN, the strongly interacting quark-gluon plasma (QGP), the matter is expected to be only existed in the universe a few microseconds after its birth [6]. From collisions of two very energetic polarized proton beams, RHIC, as the first and only polarized hadron collider in the world, discovered that from the momentum region accessible by RHIC experiments, gluons inside a longitudinally polarized fast moving proton are polarized and have a net positive polarization along the direction of the proton, equal to about 20% of the proton's helicity [7, 8]. With one proton beam polarized longitudinally, taking the advantage of the parity violation nature of the weak interaction, RHIC has performed the best measurements of the net sea quark polarization and its flavor dependence inside a polarized proton [9, 10]. With one proton beam polarized transversely, RHIC has provided and will continue providing tremendous new opportunities to probe and to study the quantum correlations between the spin direction of the proton and the preference in direction of the confined motion of quarks and gluons within the proton [11, 12]. Such quantum correlations, without any doubt, are the most sensitive to the QCD dynamics and the formation of its bound states.

The experimental measurements and discoveries by the PHENIX collaboration, along with those by the STAR collaboration and early BRAHMS and PHOBOS collaborations, have defined the RHIC science program and will continue to do so. In this short article, we briefly summarize the important and critical roles that PHENIX Experiment has played in determining the proton's internal structure, especially emphasizing the recent achievements. Some future opportunities and potentials of PHENIX Experiment for exploring the proton structure are also discussed.

2. The helicity structure of the proton

Parton distribution and correlation functions describe the fascinating relation between a fast moving proton in high energy scattering and the quarks and gluons within it. They carry rich information on proton's mysterious partonic structure that cannot be calculated by QCD perturbation theory. Parton distribution functions (PDFs) are the simplest of all correlation functions, $f_{i/p}(x, \mu^2)$, defined as the probability distributions to find a quark, an antiquark, or a gluon ($i = q, \bar{q}, g$) in the proton carrying its momentum fraction between x and $x + dx$, probed at the factorization scale μ . PDFs also play an essential role to connect the measured cross sections of colliding proton(s) to the short-distance scattering between quarks and gluons. Without them, we would not be able to understand the hard probes, cross sections with large momentum transfers, in high energy hadronic collisions, as well as the discovery of Higgs particles in proton-proton collisions at the LHC. PDFs are nonperturbative, but, universal, and have been traditionally extracted from QCD global analysis of all existing high energy scattering data in the framework of QCD factorization[13–16]. The excellent agreement between the theory and data on the scaling-violation behavior, or the factorization scale μ -dependence, of the PDFs has provided one of the most stringent tests for QCD as the theory of strong interaction.

Proton has spin $1/2$ in the unit of fundamental constant \hbar . That is, proton has a quantized finite angular momentum when it is at the rest. Proton is a composite particle made of quarks and gluons. Its spin, like its mass and other properties, is an emergent phenomenon of QCD dynamics. We do not fully understand QCD if we do not understand how quarks and gluons, and their dynamics make up the proton's spin.

The proton's spin $1/2$ was once attributed to the superposition of quark spin of three valence quarks according to the Quark Model. The proton spin puzzle (also known as the spin “crisis”) – a very little of proton's spin is carried by its quarks, discovered by European Muon Collaboration (EMC) about 30 years ago [17, 18], has led to tremendous theoretical and experimental activities to explore the proton's spin structure and to search for an answer to one of the most fundamental questions in QCD – how do the spin, the confined motion and the dynamics of quarks and gluons inside the proton make up its spin $1/2$?

2.1. The RHIC spin program

The RHIC spin program, with the only polarized proton-proton collider in the world, was designed to probe the internal quark/gluon structure of a polarized proton, and to search for the origin of and the answer to the long-standing spin puzzle. The RHIC spin program has the following three goals [19]:

- precision measurement of the polarized gluon distribution $g(x, \mu^2)$ over a large range of momentum fraction x to constrain the gluon spin contribution to the proton's spin,
- measurements of the polarized quark and anti-quark flavor structure in the proton, and
- studies of the novel transverse-spin phenomena in QCD.

Having the collisions of two high energy polarized proton beams with the polarization in either longitudinal or transverse direction, the RHIC spin program has a special advantage in probing the content of polarized gluons inside a polarized proton and the novel transverse spin phenomena in QCD. With its reach in both energy and polarization, the RHIC spin program has an unmatched capability to probe the flavor dependence of polarized sea of the proton by studying the parity violating single-spin asymmetry of W^\pm -boson production. The RHIC spin program is playing a unique and very critical role in our effort to solve the proton spin puzzle.

Proton is a composite particle of quarks and gluons, and its spin could receive contribution from the spin of quarks and gluons, as well as the orbital angular momenta of quarks and gluons due to their confined motion. Proton is also a highly dynamic quantum system of quarks and gluons full of fluctuations at all distance scales. Numbers of quarks and gluons vary at all time, given by the probability distributions to find them, such as the PDFs. Similarly, the quark and gluon spin contributions to a polarized proton are given by their helicity distributions,

$$\Delta f_{i/p}(x, \mu^2) \equiv f_{i/p}^+(x, \mu^2) - f_{i/p}^-(x, \mu^2), \quad (1)$$

defined as the difference of the probability distribution to find a parton of flavor i with the same helicity as the proton, $f_{i,p}^+$, and that of opposite helicity, $f_{i,p}^-$. The spin $1/2$ of a longitudinally polarized proton could be decomposed according to the following fundamental sum rule [20–23],

$$S_p = \frac{1}{2} = \frac{1}{2} \Delta \Sigma(\mu^2) + \Delta G(\mu^2) + (L_q(\mu^2) + L_g(\mu^2)), \quad (2)$$

where $\Delta\Sigma(\mu^2)$ and $\Delta G(\mu^2)$ are net quark and gluon helicity defined as,

$$\begin{aligned}\Delta\Sigma(\mu^2) &= \sum_{i=q,\bar{q}} \int_0^1 dx \Delta f_{i/p}(x, \mu^2) \equiv \int_0^1 dx (\Delta u + \Delta\bar{u} + \Delta d + \Delta\bar{d} + \Delta s + \Delta\bar{s})(x, \mu^2), \\ \Delta G(\mu^2) &= \int_0^1 dx \Delta f_{g/p}(x, \mu^2) \equiv \int_0^1 dx \Delta g(x, \mu^2).\end{aligned}\tag{3}$$

In Eq. (2), the factor $1/2$ in the right-hand-side of the equation is the spin of each quark and anti-quark; and $L_q(\mu^2)$ and $L_g(\mu^2)$ represent the quark and gluon orbital angular momentum contribution, respectively. The parton helicity distributions, Δf , are the key ingredients for solving the proton spin puzzle.

The experiment of inclusive electron-proton deep inelastic scattering (DIS), $\ell(k) + h(p) \rightarrow \ell'(k') + X$ with a large momentum transfer $Q \equiv \sqrt{-q^2} \equiv \sqrt{-(k - k')^2} \gg 1/\text{fm}$, discovered the quarks inside the proton in the nineteen sixties at SLAC. The same experimental setting with longitudinally polarized electron and longitudinally polarized proton can access the helicity states of quarks and gluons of the polarized proton. With the approximation of one-photon exchange between the scattering lepton and the proton, neglecting the Z -boson exchange, the difference of the polarized DIS cross sections with the proton's spin reversed measures the polarized DIS structure function, $g_1(x_B, Q^2)$, as

$$\frac{1}{2} \left[\frac{d^2\sigma^{\rightarrow\rightarrow}}{dx_B dQ^2} - \frac{d^2\sigma^{\rightarrow\leftarrow}}{dx_B dQ^2} \right] \simeq \frac{4\pi\alpha_{em}^2}{Q^4} y(2-y) g_1(x_B, Q^2),\tag{4}$$

where the terms suppressed by $x_B^2(M_p^2/Q^2)$ with proton mass M_p have been neglected, $x_B \equiv Q^2/2p \cdot q$ is the Bjorken variable, and $y = q \cdot p/k \cdot p$ is the inelasticity of DIS. In terms of QCD factorization [24], the DIS structure function g_1 can be factorized into a sum of parton helicity distributions with perturbatively calculable coefficients expressed in a power series of strong coupling α_s [25–31]. At the leading order (LO) in α_s ,

$$g_1(x_B, Q^2) = \frac{1}{2} \sum e_q^2 [\Delta q(x_B, Q^2) + \Delta\bar{q}(x_B, Q^2)],\tag{5}$$

where e_q denotes a quark's electric charge, and the resolution scale of the parton helicity distributions is set to be equal to the resolution scale of the exchange virtual photon, $\mu = Q$. It is clear from Eq. (5) that the structure function $g_1(x_B, Q^2)$ is directly sensitive to the proton's spin structure in terms of the *combined* quark and anti-quark helicity distributions. Because of the electroweak probe of the inclusive DIS measurements, the gluon helicity distribution Δg enters the expression for g_1 only at higher order in perturbation theory. Since Δg also contributes to the scaling violations (the resolution scale μ^2 -dependence) of quark and anti-quark helicity distributions, the access to gluon polarization by DIS measurements of g_1 requires a large level arm in Q^2 , which could be achieved at a future Electron-Ion Collider (EIC) [32].

With the various hadronic probes, such as jet(s) and identified hadron(s), and electroweak probes, such as the photon, lepton(s), and W/Z -bosons, the RHIC spin program and its measurements of many complementary observables provide a much more direct access to gluon polarization, as well as flavor separation of quark polarizations.

2.2. The gluon helicity structure

Longitudinally polarized proton-proton collisions at RHIC allow access to gluon helicity distribution, $\Delta g(x, \mu^2)$, at LO in perturbative QCD (pQCD). With its detector advantages, the PHENIX experiment makes the best connection to Δg via single inclusive π^0 production at large transverse momentum p_\perp by measuring the inclusive double-helicity asymmetries, A_{LL} , defined as

$$A_{LL} = \frac{\Delta\sigma}{\sigma} = \frac{\sigma_{++} - \sigma_{+-}}{\sigma_{++} + \sigma_{+-}}, \quad (6)$$

where $\Delta\sigma$ (σ) is the polarized (unpolarized) cross section, and σ_{++} (σ_{+-}) represents the cross section of $\vec{p} + \vec{p}$ collisions with the same (opposite) proton helicity. In terms of QCD factorization, both the polarized and unpolarized cross sections for the single inclusive π^0 production can be factorized to show the explicit connection to the parton helicity distributions and PDFs, respectively,

$$A_{LL}^{\pi^0} = \frac{\sum_{abc} \Delta f_{a/p}(x_1) \otimes \Delta f_{b/p}(x_2) \otimes \Delta \hat{\sigma}_{a+b \rightarrow c+X}(x_1, x_2, p_c) \otimes D_{c \rightarrow \pi^0}(z)}{\sum_{abc} f_{a/p}(x_1) \otimes f_{b/p}(x_2) \otimes \hat{\sigma}_{a+b \rightarrow c+X}(x_1, x_2, p_c) \otimes D_{c \rightarrow \pi^0}(z)}, \quad (7)$$

where x_1 and x_2 are momentum fractions of two colliding partons, $D_{c \rightarrow \pi^0}(z)$ is the fragmentation function (FF) representing a probability distribution for a parton c of momentum p_c to fragment into a hadron π^0 of momentum $z p_c$, \otimes represents the convolution over the active parton's momentum fractions, and the dependence on the factorization and renormalization scales are suppressed. In Eq. (7), $\Delta \hat{\sigma}_{a+b \rightarrow c+X}$ ($\hat{\sigma}_{a+b \rightarrow c+X}$) is the polarized (unpolarized) scattering cross section of a partonic subprocess, $a + b \rightarrow c + X$, for two active incoming partons of flavor a and b , respectively, to produce a single inclusive parton of flavor c and momentum p_c . Both polarized and unpolarized partonic cross sections are calculable in pQCD, and are available for LO as well as next-to-leading order (NLO) in powers of α_s . For the kinematic region covered by the RHIC energies, partonic cross sections of gluon initiated subprocesses are significantly larger than those initiated by quarks and antiquarks. That is, measurements of the asymmetry $A_{LL}^{\pi^0}$ by PHENIX Experiment at RHIC energies could provide very sensitive information on the gluon helicity distribution.

The factorized expression for $A_{LL}^{\pi^0}$ in Eq. (7) should be valid for all single inclusive hadron production so long as the produced hadron transverse momentum is much larger than its mass, $p_{h\perp} \gg M_h$, to ensure the validity of QCD factorization, and the π^0 FFs, $D_{c \rightarrow \pi^0}(z)$, are replaced by corresponding hadron FFs, $D_{c \rightarrow h}(z)$. This is because all factorized partonic scattering cross sections are insensitive to the details of hadronic states produced. Having the universal FFs, $D_{c \rightarrow h}(z)$, extracted from other scattering processes, such as $e^+ + e^- \rightarrow h(p_h) + X$, measurements of A_{LL}^h for the production of single inclusive hadron h other than π^0 provide additional information on the universal parton helicity distributions. The PHENIX Experiment measured the asymmetry $A_{LL}^{\pi^0}$ [8, 33–36], as well as A_{LL}^η [37].

By removing the dependence on the FFs, and replacing the single-parton inclusive cross sections, $\Delta \hat{\sigma}_{a+b \rightarrow c+X}$ and $\hat{\sigma}_{a+b \rightarrow c+X}$ by corresponding partonic jet cross sections, $\Delta \hat{\sigma}_{a+b \rightarrow \text{jet}+X}$ and $\hat{\sigma}_{a+b \rightarrow \text{jet}+X}$, respectively, the factorized expression for $A_{LL}^{\pi^0}$ in Eq. (7) reduces to the factorized expression for A_{LL}^{jet} , which depends on the same parton helicity distributions and PDFs. Precise measurements of the double longitudinal spin asymmetry for jet production

at RHIC energies could also provide excellent information on parton helicity distributions [7, 38–41].

With the earlier measurements of the double helicity asymmetry, $A_{LL}^{\pi^0}$, by the PHENIX Experiment at the mid-rapidity for $\sqrt{s} = 200$ GeV collision energy in 2005 and 2006 [33–36, 42], along with measurements of A_{LL}^{jet} by the STAR Experiment [38–41], the NLO QCD global analysis, known as the “DSSV” analysis, concluded that the RHIC data – within their uncertainties at that time – did not show any evidence of a net polarization of gluons inside the proton [43, 44].

Recently, based on data collected in 2009 at $\sqrt{s} = 200$ GeV at RHIC, which not only approximately doubles the statistics of the earlier measurements [35, 37], but also extends the range of measured p_{\perp} , PHENIX Collaboration published new measurements for both $A_{LL}^{\pi^0}$ and A_{LL}^{η} [8]. As shown in Fig. 1, three data sets collected during the 2005, 2006, and

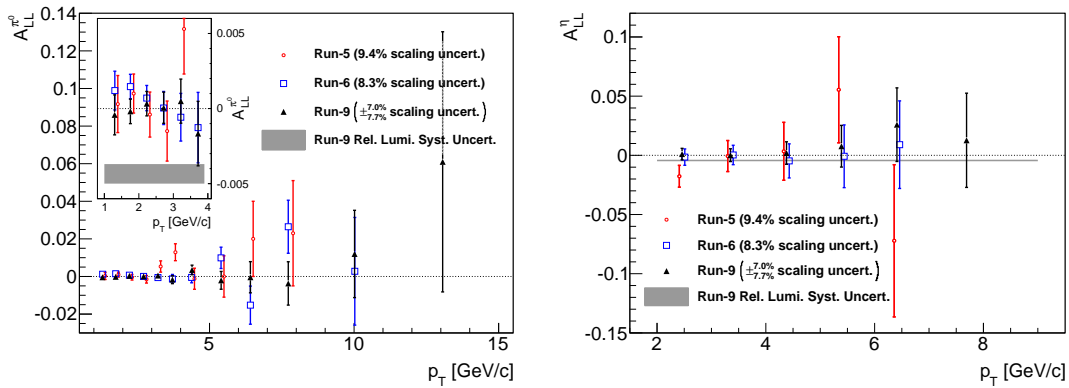


Fig. 1 $A_{LL}^{\pi^0}$ (Left) and A_{LL}^{η} (Right) as a function of meson’s transverse momentum p_T for the 2005 (red circle), 2006 (blue square) and 2009 (black triangle) PHENIX data sets.

2009 RHIC runs with polarized proton collisions are consistent with each other.

With the better statistics and extended p_{\perp} range, new data from 2009 RHIC run could naturally put tighter constraints on gluon helicity distribution, $\Delta g(x)$, and extend the range of x over which meaningful constraints can be obtained from QCD global fits. Within experimental uncertainties, the new PHENIX data on $A_{LL}^{\pi^0}$ and A_{LL}^{η} are still consistent with the existing DSSV analysis, and other recent NLO QCD global analyses of DIS-only data by Blümlein and Böttcher (BB10) [45] and Ball et. al. (NNPDF) [46, 47], as well as the analysis by Leader et. al. (LSS10) [48] based on both DIS and Semi-Inclusive DIS (SIDIS) data. Since various analyses used different assumptions on the symmetry properties of parton helicity distributions, and different functional forms for the distributions at the input scale, the determination of the gluon helicity distribution, $\Delta g(x, \mu^2)$ varies, see the detailed discussion in the PHENIX publication [8].

Although the new PHENIX data on $A_{LL}^{\pi^0}$ and A_{LL}^{η} do not show any significant asymmetry [8], the new STAR data on A_{LL}^{jet} of inclusive jet production from the same 2009 run at RHIC show a non-vanished double-spin asymmetry over the whole range $5 \lesssim p_T \lesssim 30$ GeV [7], which differs from the previous results on jet production published by the STAR Collaboration [38–40]. The most recent DSSV QCD global analysis, referred as “DSSV++” [49], shows that the new PHENIX data and STAR data are actually consistent with each other,

as shown in Fig. 2(Left). The new data sets and new DSSV++ QCD global analysis lead to a significant net positive gluon helicity contribution from the x region probed by the current measurements at RHIC, $0.05 \lesssim x \lesssim 0.2$, with a better constrained χ^2 profile for the global analysis, as shown in Fig. 2(Right). For the first time, we have a clear experimental evidence to show that gluon could give a non-vanish contribution to the proton's spin, at least from the momentum region probed by the current RHIC measurements.

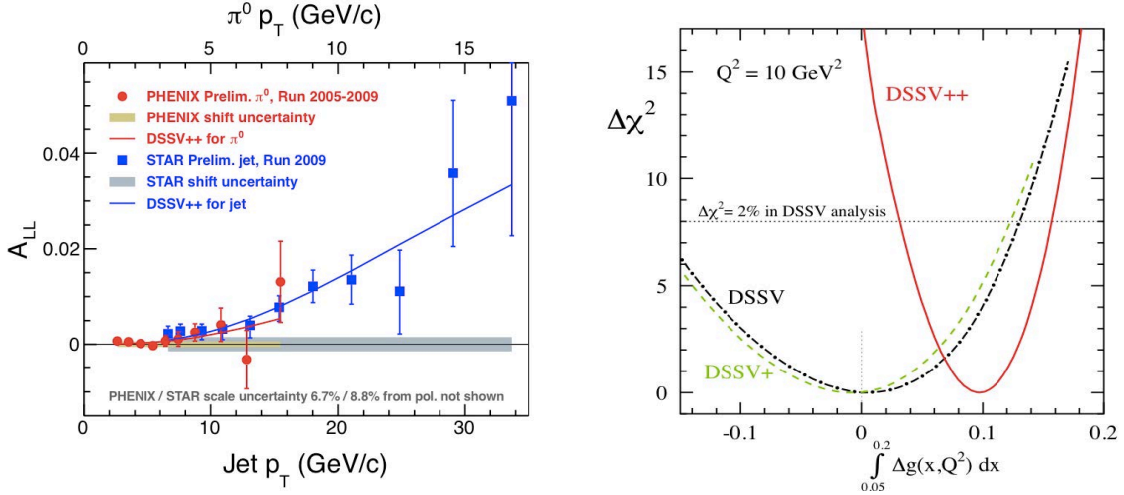


Fig. 2 Left: Double-spin asymmetry A_{LL} of new PHENIX and STAR data are compared with the new DSSV++ QCD global analysis [49]. Right: the χ^2 profile for the integrated gluon helicity contribution in the x region currently probed at RHIC for $\sqrt{s} = 200$ GeV.

With new measurements of π^0 in large forward rapidity region at $\sqrt{s} = 500$ GeV, a higher center-of-mass energy of polarized proton-proton collisions at RHIC, the PHENIX Experiment with its forward calorimeter can access the gluon helicity distribution at a momentum fraction x as small as 0.002, which will considerably improve our knowledge of the gluon spin contribution to the proton's spin in the x -range of 0.002 – 0.2 [19].

2.3. The sea quark helicity structure

The combination of the large body of inclusive DIS data has provided excellent measurements of combined quark and antiquark helicity structure, and established that the up quarks and anti-upquarks combine to have net polarization along the proton spin, whereas the down quarks and anti-downquarks combine to carry negative polarization. The “total” $\Delta u + \Delta \bar{u}$ and $\Delta d + \Delta \bar{d}$ helicity distributions are very well constrained for the medium to large x , contributing to about 30% of the proton's spin.

However, the light sea quark and anti-quark structure is still far from being well-understood [50], and its helicity distributions still carry large uncertainties, even though there are some constraints by the SIDIS data. Taking the advantage of the fact that W bosons couple only the left-handed quarks and right-handed antiquarks ($u_L \bar{d}_R \rightarrow W^+$ and $d_L \bar{u}_R \rightarrow W^-$), measuring the single longitudinal spin asymmetry, $A_L = (\sigma_+ - \sigma_-)/(\sigma_+ + \sigma_-)$, of the parity violating production of W -bosons from flipping the helicity of one of the polarized colliding protons at RHIC can probe the flavor dependence of sea quark helicity distributions, Δq and $\Delta \bar{q}$. For example, the difference of the W^+ yield from the diagram on the left in Fig. 3

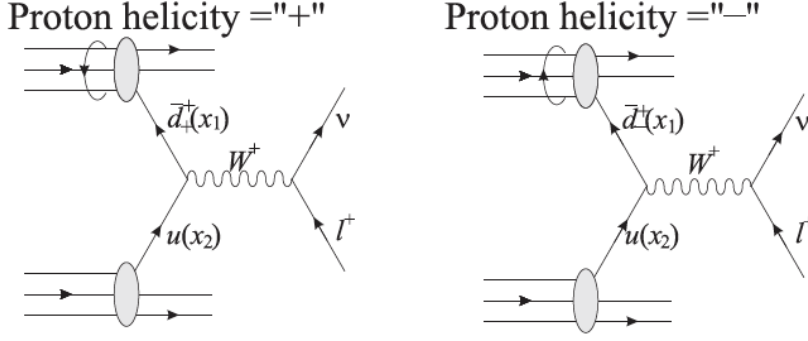


Fig. 3 Sketch for W^+ production from a leading order annihilation of a right-handed anti-downquark and a left-handed up quark in the collision of a polarized proton (top) and an unpolarized proton (bottom). The produced W^+ then decays to a positron and an electron neutrino.

and that from the diagram on the right is of good information on anti-downquark helicity distribution, $\Delta\bar{d}(x_1) = \bar{d}_+^+(x_1) - \bar{d}_-^+(x_1)$, where the subscript $+$ ($-$) indicates the positive (negative) helicity state of the polarized proton, the superscript $+$ represents the handiness of the anti-downquark, and x_1 is the momentum fraction of the polarized proton carried by the anti-downquark. Production of the W -boson requires a large momentum transfer at a scale where higher order QCD corrections can be evaluated reliably, and is free from uncertainties in fragmentation functions that are needed for probing light hadrons. The measured W -boson cross sections in unpolarized hadronic collisions at Tevatron and the LHC, as well as at RHIC, have confirmed our theoretical understanding of the production mechanism.

The measurements of A_L of W^\pm -bosons at RHIC as a function of decay lepton's transverse momentum and rapidity provide the uniquely clean information on the sea quark helicity distributions, as well as its flavor structure inside a polarized fast moving proton. With the W mass setting up the hard scale for the momentum transfer of the collisions, RHIC's W -physics program could probe the quark and anti-quark helicity distributions at a medium momentum fraction, $0.05 \lesssim x \lesssim 0.4$, providing strong constraints on the sea quark contribution to the proton's spin. Even more important, RHIC's W -physics program could provide the unique and much needed information on the sea quark helicity asymmetry, such as $\Delta\bar{d}(x) - \Delta\bar{u}(x)$, in a perfect kinematic region, in view of the puzzling sign change of unpolarized sea quark distributions, $\bar{d}(x) - \bar{u}(x)$, at $x \sim 0.3$ observed by the E886/NuSea Collaboration at Fermilab in its extraction of $\bar{d}(x) - \bar{u}(x)$ over the region $0.02 < x < 0.345$ from the measurements of Drell-Yan process [51–53]. The sea quark asymmetry in both momentum and helicity distributions is fundamentally important for understanding the proton structure.

From the background subtracted yields of positrons and electrons in p - p collisions at $\sqrt{s} = 500$ GeV at RHIC, PHENIX experiment extracted the W^+ and W^- boson production cross sections, $\sigma(pp \rightarrow W^+ X) \times BR(W^+ \rightarrow e^+ \nu_e) = 144.1 \pm 21.2(\text{stat})_{-10.3}^{+3.4}(\text{syst}) \pm 15\%(\text{norm})\text{pb}$, and $\sigma(pp \rightarrow W^- X) \times BR(W^- \rightarrow e^- \bar{\nu}_e) = 31.7 \pm 12.1(\text{stat})_{-8.2}^{+10.1}(\text{syst}) \pm 15\%(\text{norm})\text{pb}$, respectively, where BR is the W 's decay branching ratio [10]. The measurements of PHENIX Collaboration, together with that of STAR Collaboration [54], provided in fact the very first W -boson production cross sections in p - p collisions, which are consistent with earlier measurements in \bar{p} - p collisions at CERN and Fermilab [10].

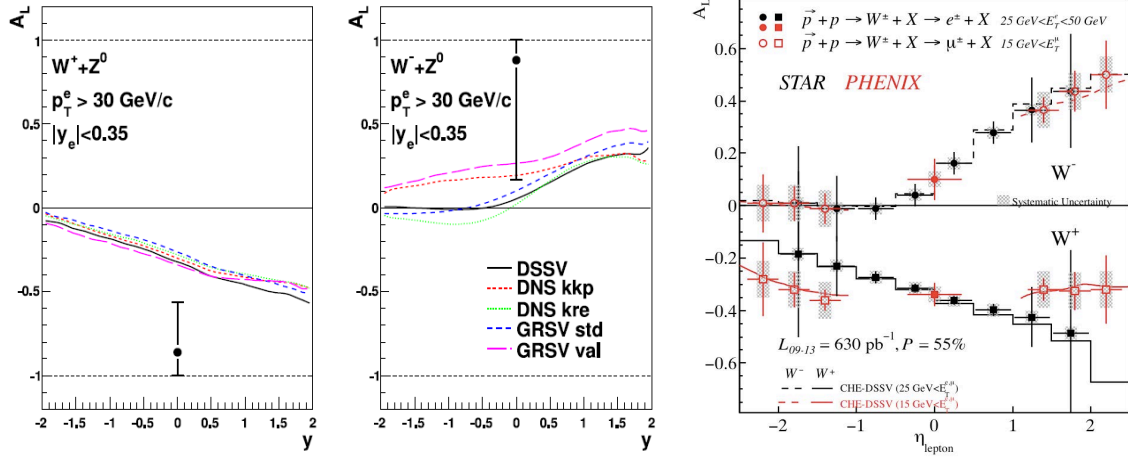


Fig. 4 PHENIX measurement of A_L for electrons (Left) and positions (Middle) from W and Z decays [10], along with theory predictions [55]. Right: Expected uncertainties for A_L of W^\pm production for PHENIX and STAR after the 2013 run. The asymmetries have been randomized around the central value of DSSV analysis.

With its early data on leptonic W decay in polarized p - p collisions at $\sqrt{s} = 500$ GeV, RHIC's W -physics program started to impact our understanding of proton's polarized sea structure [9, 56]. In Fig. 4, the very first PHENIX measurement of the parity violating single spin asymmetry, A_L , of electrons (Left) and positions (Right) from W and Z decays are presented [10]. Although the experimental uncertainties are clearly large, the asymmetries are consistent with the early theory expectations.

With the new STAR data on $A_L^{W^\pm}$ [9], and the expected experimental uncertainties for A_L measurements of both PHENIX and STAR from the recent polarized p - p runs at RHIC [19], as shown in Fig. 4 (Right), new and updated DSSV global analyses of parton helicity distributions clearly indicate that the sea quark structure shows hints of not being SU(2)-flavor symmetric: the $\Delta\bar{u}$ distribution has a tendency to be mainly positive, and the $\Delta\bar{d}$ anti-quarks likely carry an opposite polarization. From the χ^2 profiles of the global fits in

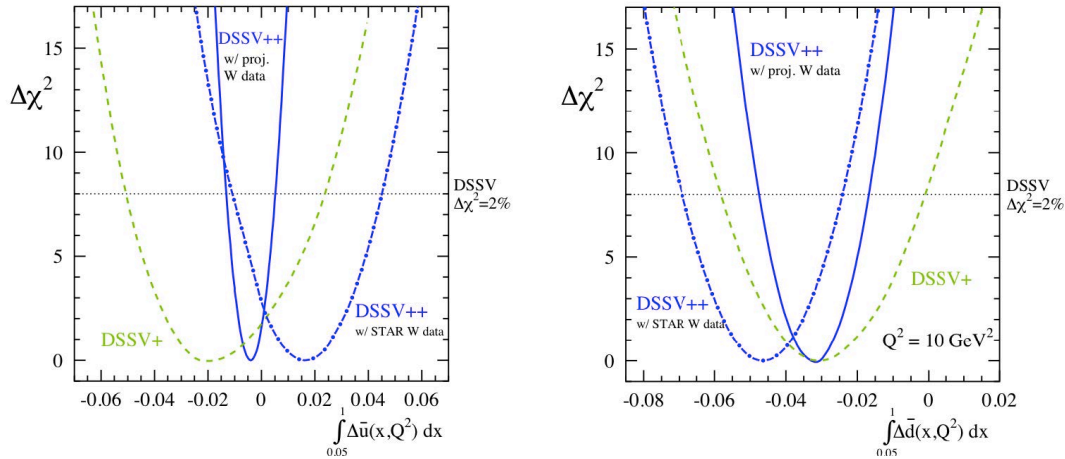


Fig. 5 Expected χ^2 profiles from DSSV global analyses of parton helicity distributions for $\Delta\bar{u}$ (left) and $\Delta\bar{d}$ (right): DSSV+ with new SIDIS data, and DSSV++ with new STAR data or with projected data on A_L of W^\pm boson production in Fig. 4 (Right).

Fig. 5, the new RHIC data on the parity violating single spin asymmetries will provide a powerful constraint on the sea quark structure and its contribution to the proton's spin.

QCD global analyses of all available data from DIS, SIDIS, and RHIC have provided good information on quark/gluon helicity structure of a polarized fast moving proton, and quark/gluon spin contribution to the proton's spin [32]. From the region of momentum fractions accessible by existing experimental measurements, the net helicity of quarks and antiquarks combined could account for about 30% of proton's spin, while gluons are likely to give a positive contribution to the proton's spin, close to 20% from the most recent RHIC data, but with a huge uncertainty from the region of gluon momentum fractions that is not available to all existing and near future facilities [49]. While we need the final word of the gluon spin contribution to the proton's spin from the proposed future EIC [32], it is fundamentally important to investigate the confined transverse motion of quarks and gluons inside a fast moving proton, and their contribution to the proton's spin.

3. Transverse parton structure of the proton

To have a direct access to the transverse parton structure of a fast moving proton in high energy scattering requires a new type of physical observables – the controlled probes that have at least two distinctive momentum scales: a large scale $Q \gg \Lambda_{\text{QCD}} \sim 1/\text{fm}$ to localize the probes to “see” the particle nature of quarks and gluons, and a small scale $q \ll Q$ to be sensitive to the confined transverse motion or spatial distribution of quarks and gluons inside the proton.

Theoretically, the simplest transverse parton structure of the proton could be characterized by the Wigner distributions $W_{i/p}(x, \mathbf{k}_T, \mathbf{b}_T)$ – the probability distributions to find a parton of flavor $i (= q, \bar{q}, g)$ inside the fast moving proton, carrying its momentum fraction between x and $x + dx$ and having a transverse momentum \mathbf{k}_T at a transverse spatial position \mathbf{b}_T with respect to its center [57]. More complex transverse parton structure of the proton could be represented by multi-parton correlation functions in terms of longitudinal momentum fractions, transverse momenta and positions of all active partons. Although the Wigner distributions are used extensively in other branches of physics [58], there has not been any known way to measure the quark and gluon Wigner distributions in high energy experiments.

However, various reductions of the Wigner distributions could be probed in high energy experiments [32]. By integrating over \mathbf{b}_T , the Wigner distributions are reduced to the three-dimensional (3D) momentum distributions of quarks and gluons inside the fast moving proton – transverse momentum dependent PDFs (TMDs), $f_{i/p}(x, \mathbf{k}_T)$; and the TMDs could be further reduced to the better known PDFs, $f_{i/p}(x, \mu^2)$ by integrating over \mathbf{k}_T with a proper ultraviolet (UV) renormalization when $\mathbf{k}_T \rightarrow \infty$ for the quark/gluon operators defining the PDFs at the renormalization scale μ . Similarly, by integrating over \mathbf{k}_T , the Wigner distributions are reduced to the impact parameter distributions, $f_{i/p}(x, \mathbf{b}_T)$, the probability distributions to find a parton of flavor i and momentum fraction x at a transverse spatial position \mathbf{b}_T , which are effectively the tomographic images of quarks and gluons inside the proton. Furthermore, by taking the Fourier transform of \mathbf{b}_T into the conjugate momentum Δ_T , $f_{i/p}(x, \mathbf{b}_T)$ could be transformed into the generalized PDFs (GPDs), such as $H_{i/p}(x, \xi, t)$ and $E_{i/p}(x, \xi, t)$ at $\xi = 0$ with $t = -\Delta_T^2$ [59]. The GPDs could be extracted from measurements of exclusive processes in lepton-hadron DIS or in ultra-peripheral hadronic collisions. The TMDs and GPDs represent various aspects of the same proton's transverse structure of

quarks and gluons that could be probed in high energy scattering [32]. In fact, some GPDs are intimately connected with the orbital angular momentum carried by quarks and gluons [60]. The Ji's sum rule is one of the examples that quantify this connection [21],

$$J_q = \frac{1}{2} \lim_{t \rightarrow 0} \int_0^1 dx x [H_q(x, \xi, t) + E_q(x, \xi, t)] , \quad (8)$$

which represents the total angular momentum J_q (including both helicity and orbital contributions) carried by quarks and anti-quarks of flavor q . A similar relation holds for gluons.

With the polarized high energy proton beam(s), the RHIC spin program could access the proton's transverse structure of quarks and gluons by measuring various TMDs, as well as GPDs via exclusive processes in ultra-peripheral p - p and p - A collisions. The RHIC spin program could measure many emergent QCD phenomena, such as quantum correlations between the proton's spin direction and preference of the confined transverse motion of quarks and gluons inside the polarized proton, known as the Sivers effect [61]. Furthermore, it could probe quantum correlation between the spin direction of the fragmenting parton and preference in direction where the produced hadron emerges, known as the Collins effect [62].

3.1. Transverse single-spin asymmetry – A_N

Transverse single-spin asymmetry (SSA), $A_N \equiv (\sigma(s_T) - \sigma(-s_T))/(\sigma(s_T) + \sigma(-s_T))$, is defined as the ratio of the difference and the sum of the cross sections when the spin of one of the identified hadron s_T is flipped. Large SSAs of inclusive single pion production with a large momentum transfer in hadronic collisions have been consistently observed since nineteen seventies, as shown in Fig. 6, although the asymmetries were once thought impossible in QCD [63]. With over two decades of intense theoretical as well as experimental efforts, our understanding of the observed large SSAs in QCD has been much improved. Large SSAs are not only possible in QCD, but also carry extremely valuable information on the transverse motion and structure of quarks and gluons inside a transversely polarized proton.

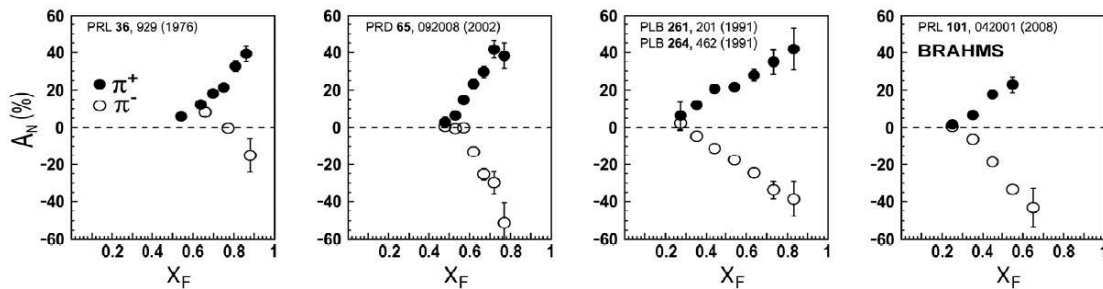


Fig. 6 Persistent transverse single-spin asymmetry, A_N , in hadronic single inclusive pion production.

From the parity and time-reversal invariance of QCD dynamics, non-vanish transverse SSAs are necessarily connected to the transverse momentum of quarks and gluons inside the transversely polarized proton [64]. Two complementary QCD-based approaches have been proposed to describe the physics behind the measured SSAs: the TMD factorization approach

[61, 62, 65, 66] and the collinear factorization approach [67–72]. In the TMD factorization approach, the asymmetry is attributed to direct correlation between spin and transverse momentum, which are represented by the TMD PDFs or FFs, such as the Sivers and Collins functions, respectively. On the other hand, the asymmetry in the collinear factorization approach is generated by twist-3 collinear PDFs or FFs. With the transverse momenta of all active partons integrated, the explicit spin-transverse momentum correlation in the TMD approach is now replaced by the integrated net effect of spin-transverse momentum correlations, which are effectively generated by QCD color Lorentz force [73].

Two approaches each have their own kinematic domain of validity, while they are consistent with each other in the perturbative regime where they both apply [74–78]. The TMD factorization approach is more suitable for evaluating the SSAs of scattering processes with two very different momentum transfers, $Q \gg q \gtrsim \Lambda_{\text{QCD}}$, while the collinear factorization approach is more relevant to the SSAs of scattering cross sections with all observed momentum transfers hard and comparable: $Q' \sim Q \gg \Lambda_{\text{QCD}}$. In hadronic collisions, the single inclusive hadron production at high p_T is better treated in the collinear factorization approach, while the Drell-Yan and W/Z production at a low transverse momentum, $q_T \ll Q$, needs the TMD factorization approach.

3.2. A_N of single hadron production

The inclusive single hadron production at large transverse momentum p_T at RHIC has effectively one large momentum transfer at $\mathcal{O}(p_T) \gg \Lambda_{\text{QCD}}$. Collinear factorization approach is more suited for studying the transverse SSAs of the inclusive single hadron production. In terms of the collinear factorization, the transverse SSAs are effectively power suppressed observables comparing to the production cross sections. That is, the asymmetries are in general small, except in the region of phase space where the momentum spectrum of the observed pions is very steep, and a small shift in the spectrum could make the difference of two cross sections with the proton spin flipped to be comparable with the cross section itself, leading to a significant value of the asymmetry.

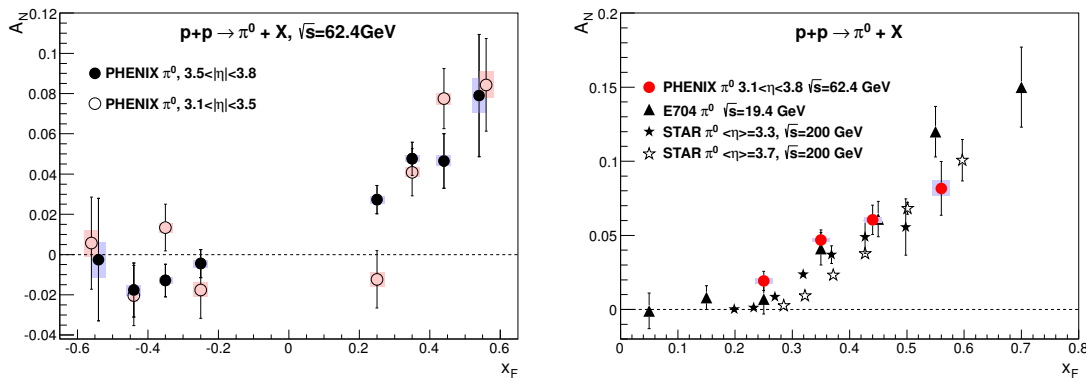


Fig. 7 $A_N^{\pi^0}$ as a function of x_F at $\sqrt{s} = 62.4$ GeV (Left) measured by PHENIX Experiment, and at various center-of-mass energies in hadronic collisions (Right).

The left plot in Fig. 7 shows $A_N^{\pi^0}$ at $\sqrt{s} = 62.4$ GeV measured by PHENIX Collaboration with the PHENIX detector at RHIC [12]. While there is a significant, nonzero asymmetry rising with $x_F > 0$ in the forward direction of the polarized proton beam, no such behavior

can be seen at negative $x_F < 0$ where the asymmetries are consistent with zero. The typical transverse momentum of these data is relatively low, over the range of $0.5 < p_T < 1$ GeV [12]. In Fig. 7 (Right), the PHENIX data of $A_N^{\pi^0}$ at $\sqrt{s} = 62.4$ GeV are compared with the measurements by Fermilab E704 at $\sqrt{s} = 19.4$ GeV and those by STAR Collaboration at $\sqrt{s} = 200$ GeV. Although these measurements were carried out with slightly different detector acceptances, there is a general agreement between the x_F dependence of nonvanishing asymmetries. The observed asymmetries appear to be independent of the center-of-mass energy of the collisions, which varies over one order of magnitude from $\sqrt{s} = 19.4$ GeV to 200 GeV. The data set plotted in Fig. 7 (Right) also covered an interesting range of transverse momentum of the observed pions from a semi-hard scale at $p_T \sim 0.5$ GeV to a hard scale at $p_T > 2$ GeV for the STAR data [11].

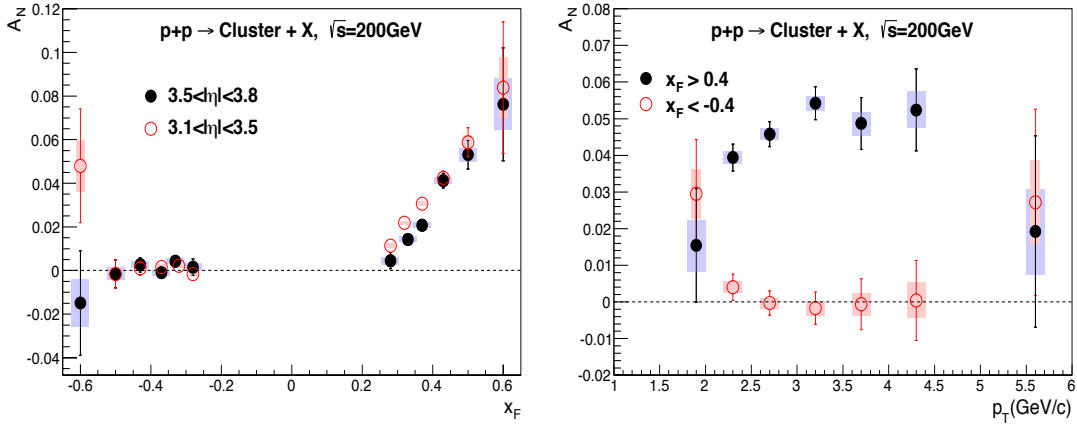


Fig. 8 A_N^{Cluster} as a function of the cluster's Feynman parameter x_F (Left) and transverse momentum p_T (Right) measured by PHENIX Collaboration at $\sqrt{s} = 200$ GeV at RHIC [12].

By resolving the two electromagnetic clusters from the two photons of $\pi^0 \rightarrow \gamma + \gamma$ decay, PHENIX detector is capable of detecting π^0 with its energy, $E_{\pi^0} \lesssim 20$ GeV. However, with increasing energy, the opening angle between the two photons becomes so small that their electromagnetic clusters fully merge in the PHENIX detector. The reconstruction of π^0 from the two-gamma decay mode limits the x_F range to below 0.2 at $\sqrt{s} = 200$ GeV, where transverse SSAs are small. To overcome this limitation, the data analysis of transverse SSAs is also done for inclusive electromagnetic clusters [12]. The clusters are dominated from $\pi^0 \rightarrow \gamma + \gamma$, with some contributions from direct and other photons and decay of η and other charged particles. The detailed discussion on the decomposition of the clusters can be found in Ref. [12].

The left plot in Fig. 8 summarizes the x_F -dependence of the cluster A_N for two different pseudorapidity ranges. Within statistical uncertainties the asymmetries in the forward direction of the polarized proton A_N rises almost linearly with x_F , while the asymmetries in the backward direction $x_F < 0$ are found to be consistent with zero. The non-vanish asymmetries in the forward region are of similar size compared to the π^0 asymmetries at other center-of-mass energies as shown in Fig. 7 (Right), which should not be too surprising since the inclusive electromagnetic clusters in this momentum regime are mainly formed by the photons from π^0 decay.

The right plot in Fig. 8 presents the cluster A_N , as a function of transverse momentum p_T for values of $|x_F| > 0.4$ [12]. The asymmetry rises smoothly and then seems to saturate above $p_T > 3$ GeV/c. When $p_T = 0$, A_N should vanish from the symmetry, and is expected to rise with p_T when p_T is relatively small. Since transverse SSAs of the single inclusive hadron production are intrinsically a power suppressed observable at large p_T , the A_N is expected to decrease when p_T becomes sufficiently large [69, 74]. Explicit calculations of A_N in collinear factorization approach indicates, $A_N \propto p_T/\hat{u}$, and consequently, the asymmetry does not fall as quickly as $1/p_T$ in the forward region when $x_F \gtrsim x_T = 2p_T/\sqrt{s}$ [71]. The p_T dependence of the A_N should be sensitive to the underline dynamics generating the transverse SSAs. Again, asymmetries in the negative x_F region are found to be consistent with zero within statistical uncertainties. The transverse SSAs of single inclusive hadron or inclusive cluster measured by PHENIX Experiment are consistent with those measured by STAR collaboration at RHIC.

3.3. A_N of Drell-Yan (γ^* and W/Z) production

The observed transverse SSAs of single inclusive hadron production could be generated by the spin-motion correlations and/or coherent multiple interactions before and/or after the hard collision [71]. That is, in the terminology of TMD factorization approach, both the Siverson-like (before) and the Collins-like (after) effects are responsible for the observed asymmetries. Assuming the correlation before the hard collision dominates the observed asymmetry in the inclusive pion production could actually lead to a sign puzzle for the relation between the Siverson function and the corresponding twist-3 quark-gluon correlation functions [79]. Apparently, the Collins-like correlations after the hard collision is very important for understanding the transverse SSAs in p - p collisions, as well as resolving the sign puzzle [80]. Without being able to disentangle different effects, it is difficult, if not impossible, to fully understand the physics and the mechanism to generate the novel phenomena of transverse SSAs.

Unlike the single inclusive hadron production in hadronic collision, Drell-Yan massive lepton pair production, either via a virtual photon or a W/Z boson, could have two natural and distinctive momentum scales: the invariant mass of the lepton pair, Q ($\sim M_{W/Z}$) and the transverse momentum of the pair, q_T . The most events have the strong ordering of these two scales, $Q \gg q_T$, which is natural for applying the TMD factorization approach to probe the transverse motion of quarks directly. Since the vector bosons or their decay leptons do not interact strongly after they are produced, Drell-Yan process is ideal for study the initial-state TMDs, such as Siverson functions [50].

One of the key differences between the QCD collinear factorization approach and QCD TMD factorization approach to the high energy scattering process is the universality of the non-perturbative long-distance physics. Within the collinear factorization approach, all non-perturbative long-distance physics are represented by universal (process independent) hadronic matrix elements whose operators are made of quark/gluon correlators that are effectively *localized* in space to the size of the hard collision $\sim 1/Q \ll 1/\text{fm}$. The non-perturbative long-distance physics in the TMD factorization approach is represented by TMDs. The existing definitions of TMDs involve quark-gluon correlators with *non-local* gauge links covering infinite size in space [81]. It is the non-local nature of the TMDs that led to their potential process-dependence, such as the sign change of the Siverson function extracted from SIDIS

in comparison with that extracted from the Drell-Yan process [66]. This non-universality is a fundamental prediction from the gauge invariance of QCD and the TMD factorization approach. The experimental test of this sign change is one of the open questions in hadronic physics and will provide a direct verification of QCD TMD factorization.

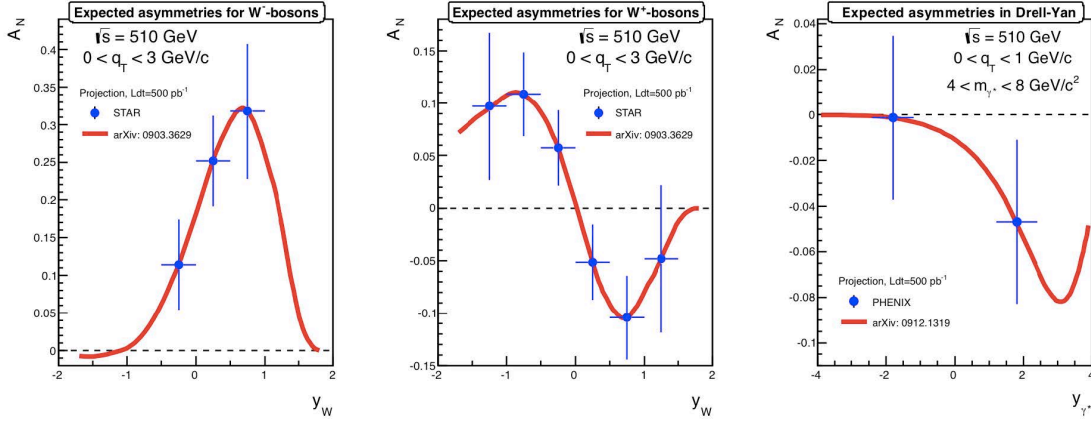


Fig. 9 A_N of Drell-Yan like process with a reconstructed W^+ (Left), W^- (Middle), or a virtual photon (Right), as a function of vector boson’s rapidity in \vec{p} - p collisions at RHIC. Also plotted are theoretical predictions based on Siivers functions extracted from low energy SIDIS measurements [82].

With the high energy polarized proton beams, RHIC can produce W and Z^0 with relatively low transverse momentum $q_T \ll M_{W/Z}$. The transverse spin program at RHIC has the unique advantage to measure the Siivers effect in the Drell-Yan like process at a true hard scale – mass of W/Z bosons. Figure 9 shows the expected uncertainties for transverse SSAs of reconstructed W^\pm (Left, Middle) and Drell-Yan production (Right) from STAR and PHENIX measurements [19]. Also plotted curves are theoretical predictions based on our knowledges of Siivers functions from SIDIS measurements [82]. These asymmetries provide an essential test for the fundamental QCD prediction of a sign change of the Siivers function in hadronic collisions with respect to that in SIDIS, as well as a test of our understanding of scale dependence (or evolution) of the Siivers functions.

Transverse SSAs and their x_F and p_T dependence in hadronic collisions are well-established, and they are emergent phenomena QCD dynamics. Along with the transverse spin programs at JLab12 and at COMPASS, the transverse spin program at RHIC with its PHENIX and STAR detectors opens up a new domain of QCD dynamics, sensitive to the confined motion, as well as the quantum correlation between the motion and intrinsic particle property, such as spin, of quarks and gluons inside a QCD bound state, like the proton. It also provides controllable and promising access to the transverse structure of the proton.

4. Summary and outlook

Proton is a dynamic system of confined quarks and gluons. Proton itself is an emergent phenomenon of QCD dynamics. Proton structure is dynamic as well. Probability distributions to find quarks and gluons, and their correlations inside the proton are fundamental,

corresponding to various aspects of the dynamic and complex system of the proton. Our knowledge of proton's internal structure is still very limited, although we have learned a lot with the advances of accelerator and detector technologies, as well as theoretical breakthroughs to identify the controllable probes to “connect” the quarks and gluons inside the proton to the leptons and hadrons observed in modern detectors.

RHIC, with the only polarized proton-proton collider in the world and the PHENIX and STAR detectors, has helped address open questions concerning the proton structure, and identified new open questions, puzzles and challenges. The PHENIX Experiment, along with STAR Experiment, has played critical roles in defining the RHIC physics program and in extracting valuable information for determining proton's internal structure. The PHENIX Experiment helps determine the helicity structure of the proton, in particular, the extraction of gluon and sea quark helicity structure inside a polarized fast moving proton, by measuring A_{LL} of single inclusive hadron production, as well as the parity violating A_L of W^\pm production. By measuring A_N of many observables, including the production of π^0 , η , direct photon, W/Z bosons, J/ψ , and the innovative inclusive electromagnetic clusters, the PHENIX Experiment help define and explore the richness and excitements of the RHIC transverse spin program.

With the upcoming p - A run at RHIC, the PHENIX Experiment will help open a new frontier of QCD to explore the fundamental nuclear structure in terms of quarks and gluons. With the help of the polarized proton beam, the PHENIX Experiment could search for the imprint of spin correlations among the nucleons inside a nucleus, without seeing nucleon, but, quarks and gluons. With the future upgrades of the PHENIX detector to sPHENIX and to fsPHENIX, the PHENIX Experiment could be even more powerful in delivering new and accurate measurements helping explore the internal structure of the proton.

Acknowledgment

We thank Abhay Deshpande for helpful discussions concerning PHENIX measurements. This work was supported in part by the U. S. Department of Energy under Contract No. DE-AC02-98CH10886, and the National Science Foundation under Grants No. PHY-0969739 and No. PHY-1316617.

References

- [1] N. Brambilla, S. Eidelman, P. Foka, S. Gardner, A.S. Kronfeld, et al., Eur.Phys.J., **C74**(10), 2981 (2014), arXiv:1404.3723.
- [2] Elliott D. Bloom, D.H. Coward, H.C. DeStaebler, J. Drees, Guthrie Miller, et al., Phys.Rev.Lett., **23**, 930–934 (1969).
- [3] Martin Breidenbach, Jerome I. Friedman, Henry W. Kendall, Elliott D. Bloom, D.H. Coward, et al., Phys.Rev.Lett., **23**, 935–939 (1969).
- [4] H. Fritzsch, Murray Gell-Mann, and H. Leutwyler, Phys.Lett., **B47**, 365–368 (1973).
- [5] RHIC homepage: <http://www.bnl.gov/rhic/> ().
- [6] M. Gyulassy and L. McLerran, Nucl. Phys., **A750**, 30 (2005).
- [7] L. Adamczyk et al. (2014), arXiv:1405.5134.
- [8] A. Adare et al., Phys.Rev., **D90**, 012007 (2014), arXiv:1402.6296.
- [9] L. Adamczyk et al., Phys.Rev.Lett., **113**, 072301 (2014), arXiv:1404.6880.
- [10] A. Adare et al., Phys. Rev. Lett., **106**, 062001 (2011), arXiv:1009.0505.
- [11] B.I. Abelev et al., Phys.Rev.Lett., **101**, 222001 (2008), arXiv:0801.2990.
- [12] A. Adare et al., Phys.Rev., **D90**, 012006 (2014), arXiv:1312.1995.
- [13] Jun Gao, Marco Guzzi, Joey Huston, Hung-Liang Lai, Zhao Li, et al., Phys.Rev., **D89**(3), 033009 (2014), arXiv:1302.6246.

-
- [14] A.D. Martin, W.J. Stirling, R.S. Thorne, and G. Watt, *Eur.Phys.J.*, **C63**, 189–285 (2009), arXiv:0901.0002.
 - [15] Richard D. Ball, Valerio Bertone, Francesco Cerutti, Luigi Del Debbio, Stefano Forte, et al., *Nucl.Phys.*, **B849**, 296–363 (2011), arXiv:1101.1300.
 - [16] S. Alekhin, J. Bluemlein, and S. Moch, *Phys.Rev.*, **D89**, 054028 (2014), arXiv:1310.3059.
 - [17] J. Ashman et al., *Phys. Lett.*, **B206**, 364 (1988).
 - [18] J. Ashman et al., *Nucl. Phys.*, **B328**, 1 (1989).
 - [19] E.C. Aschenauer, A. Bazilevsky, K. Boyle, K.O. Eyser, R. Fatemi, et al. (2013), arXiv:1304.0079.
 - [20] R. L. Jaffe and Aneesh Manohar, *Nucl. Phys.*, **B337**, 509–546 (1990).
 - [21] Xiang-Dong Ji, *Phys. Rev. Lett.*, **78**, 610–613 (1997), hep-ph/9603249.
 - [22] Masashi Wakamatsu, *Int.J.Mod.Phys.*, **A29**, 1430012 (2014), arXiv:1402.4193.
 - [23] Xiangdong Ji, Xiaonu Xiong, and Feng Yuan, *Phys. Rev. Lett.*, **109**, 152005 (2012), arXiv:1202.2843.
 - [24] John C. Collins, Davison E. Soper, and George F. Sterman, *Adv.Ser.Direct.High Energy Phys.*, **5**, 1–91 (1988), arXiv:hep-ph/0409313.
 - [25] Yuri L. Dokshitzer, *Sov. Phys. JETP*, **46**, 641–653 (1977).
 - [26] V.N. Gribov and L.N. Lipatov, *Sov. J. Nucl. Phys.*, **15**, 438–450 (1972).
 - [27] Guido Altarelli and G. Parisi, *Nucl. Phys.*, **B126**, 298 (1977).
 - [28] E.B. Zijlstra and W.L. van Neerven, *Nucl. Phys.*, **B417**, 61–100 (1994).
 - [29] R. Mertig and W.L. van Neerven, *Z. Phys.*, **C70**, 637–654 (1996), arXiv:hep-ph/9506451.
 - [30] Werner Vogelsang, *Phys. Rev.*, **D54**, 2023–2029 (1996), arXiv:hep-ph/9512218.
 - [31] A. Vogt, S. Moch, M. Rogal, and J.A.M. Vermaseren, *Nucl. Phys. Proc. Suppl.*, **183**, 155–161 (2008), arXiv:0807.1238.
 - [32] A. Accardi, J.L. Albacete, M. Anselmino, N. Armesto, E.C. Aschenauer, et al. (2012), arXiv:1212.1701.
 - [33] S.S. Adler et al., *Phys. Rev. Lett.*, **93**, 202002 (2004), arXiv:hep-ex/0404027.
 - [34] A. Adare et al., *Phys. Rev.*, **D76**, 051106 (2007), arXiv:0704.3599.
 - [35] A. Adare et al., *Phys. Rev. Lett.*, **103**, 012003 (2009), arXiv:0810.0694.
 - [36] A. Adare et al., *Phys.Rev.*, **D79**, 012003 (2009), arXiv:0810.0701.
 - [37] A. Adare et al., *Phys.Rev.*, **D83**, 032001 (2011), arXiv:1009.6224.
 - [38] B.I. Abelev et al., *Phys. Rev. Lett.*, **97**, 252001 (2006), arXiv:hep-ex/0608030.
 - [39] B.I. Abelev et al., *Phys. Rev. Lett.*, **100**, 232003 (2008), arXiv:0710.2048.
 - [40] M. Sarsour, *AIP Conf. Proc.*, **1149**, 389–392 (2009), arXiv:0901.4061.
 - [41] Pibero Djawotho, *J. Phys. Conf. Ser.*, **295**, 012061 (2011).
 - [42] B.I. Abelev et al., *Phys. Rev.*, **D80**, 111108 (2009), arXiv:0911.2773.
 - [43] Daniel de Florian, Rodolfo Sassot, Marco Stratmann, and Werner Vogelsang, *Phys. Rev. Lett.*, **101**, 072001 (2008), arXiv:0804.0422.
 - [44] Daniel de Florian, Rodolfo Sassot, Marco Stratmann, and Werner Vogelsang, *Phys. Rev.*, **D80**, 034030 (2009), arXiv:0904.3821.
 - [45] Johannes Blumlein and Helmut Bottcher, *Nucl.Phys.*, **B841**, 205–230 (2010), arXiv:1005.3113.
 - [46] Richard D. Ball et al., *Nucl.Phys.*, **B874**, 36–84 (2013), arXiv:1303.7236.
 - [47] Richard D. Ball, Valerio Bertone, Stefano Carrazza, Christopher S. Deans, Luigi Del Debbio, et al., *Nucl.Phys.*, **B867**, 244–289 (2013), arXiv:1207.1303.
 - [48] Elliot Leader, Aleksander V. Sidorov, and Dimiter B. Stamenov, *Phys.Rev.*, **D82**, 114018 (2010), arXiv:1010.0574.
 - [49] Daniel de Florian, Rodolfo Sassot, Marco Stratmann, and Werner Vogelsang, *Phys.Rev.Lett.*, **113**, 012001 (2014), arXiv:1404.4293.
 - [50] Jen-Chieh Peng and Jian-Wei Qiu, *Prog.Part.Nucl.Phys.*, **76**, 43–75 (2014), arXiv:1401.0934.
 - [51] E.A. Hawker et al., *Phys.Rev.Lett.*, **80**, 3715–3718 (1998), arXiv:hep-ex/9803011.
 - [52] J.C. Peng et al., *Phys.Rev.*, **D58**, 092004 (1998), arXiv:hep-ph/9804288.
 - [53] R.S. Towell et al., *Phys.Rev.*, **D64**, 052002 (2001), arXiv:hep-ex/0103030.
 - [54] Ross Corliss, *Phys.Part.Nucl.*, **45**, 70–72 (2014).
 - [55] Daniel de Florian and Werner Vogelsang, *Phys. Rev.*, **D81**, 094020 (2010), arXiv:1003.4533.
 - [56] C. Gal, *Phys.Part.Nucl.*, **45**, 76–78 (2014).
 - [57] Andrei V. Belitsky, Xiang-Dong Ji, and Feng Yuan, *Phys. Rev.*, **D69**, 074014 (2004), arXiv:hep-ph/0307383.
 - [58] M. Hillery, R.F. O’Connell, M.O. Scully, and Eugene P. Wigner, *Phys. Rept.*, **106**, 121–167 (1984).
 - [59] Dieter Mueller (2014), arXiv:1405.2817.
 - [60] Matthias Burkardt and Gunar Schnell, *Phys. Rev.*, **D74**, 013002 (2006), hep-ph/0510249.
 - [61] Dennis W. Sivers, *Phys.Rev.*, **D41**, 83 (1990).
 - [62] John C. Collins, *Nucl.Phys.*, **B396**, 161–182 (1993), arXiv:hep-ph/9208213.
 - [63] Gordon L. Kane, J. Pumplin, and W. Repko, *Phys.Rev.Lett.*, **41**, 1689 (1978).
 - [64] Jian-Wei Qiu and George F. Sterman, *AIP Conf.Proc.*, **223**, 249–254 (1991).

-
- [65] Stanley J. Brodsky, Dae Sung Hwang, and Ivan Schmidt, Phys. Lett., **B530**, 99–107 (2002).
 - [66] John C. Collins, Phys. Lett., **B536**, 43–48 (2002).
 - [67] A.V. Efremov and O.V. Teryaev, Sov.J.Nucl.Phys., **36**, 140 (1982).
 - [68] A.V. Efremov and O.V. Teryaev, Phys.Lett., **B150**, 383 (1985).
 - [69] Jian-Wei Qiu and George F. Sterman, Phys.Rev.Lett., **67**, 2264–2267 (1991).
 - [70] Jian-Wei Qiu and George F. Sterman, Nucl.Phys., **B378**, 52–78 (1992).
 - [71] Jian-Wei Qiu and George F. Sterman, Phys.Rev., **D59**, 014004 (1998), arXiv:hep-ph/9806356.
 - [72] Chris Kouvaris, Jian-Wei Qiu, Werner Vogelsang, and Feng Yuan, Phys.Rev., **D74**, 114013 (2006), arXiv:hep-ph/0609238.
 - [73] Jian-Wei Qiu and George F. Sterman, In *Brookhaven 1993, Future directions in particle and nuclear physics at multi-GeV hadron beam facilities*, Brookhaven National Lab, Upton, NY (1993).
 - [74] Xiangdong Ji, Jian-Wei Qiu, Werner Vogelsang, and Feng Yuan, Phys. Rev. Lett., **97**, 082002 (2006).
 - [75] Xiangdong Ji, Jian-Wei Qiu, Werner Vogelsang, and Feng Yuan, Phys.Rev., **D73**, 094017 (2006), arXiv:hep-ph/0604023.
 - [76] Xiangdong Ji, Jian-Wei Qiu, Werner Vogelsang, and Feng Yuan, Phys.Lett., **B638**, 178–186 (2006), arXiv:hep-ph/0604128.
 - [77] Yuji Koike, Werner Vogelsang, and Feng Yuan, Phys.Lett., **B659**, 878–884 (2008), arXiv:0711.0636.
 - [78] Alessandro Bacchetta, Daniel Boer, Markus Diehl, and Piet J. Mulders, JHEP, **08**, 023 (2008).
 - [79] Zhong-Bo Kang, Jian-Wei Qiu, Werner Vogelsang, and Feng Yuan, Phys.Rev., **D83**, 094001 (2011), arXiv:1103.1591.
 - [80] Koichi Kanazawa, Yuji Koike, Andreas Metz, and Daniel Pitonyak, Phys.Rev., **D89**(11), 111501 (2014), arXiv:1404.1033.
 - [81] John C. Collins and Ted C. Rogers, Phys.Rev., **D87**(3), 034018 (2013), arXiv:1210.2100.
 - [82] Zhong-Bo Kang and Jian-Wei Qiu, Phys.Rev., **D81**, 054020 (2010), arXiv:0912.1319.